

## Surface-Enhanced Raman Scattering Studies on Aggregated Gold Nanorods<sup>†</sup>

Babak Nikoobakht and Mostafa A. El-Sayed\*

Laser Dynamics Laboratory, School of Chemistry and Biochemistry, Georgia Institute of Technology, Atlanta, Georgia 30332-0400

Received: August 15, 2002; In Final Form: February 24, 2003

Surface-enhanced Raman scattering (SERS) of adsorbed molecules on gold nanorods (NRs) with dimensions of 10 nm × 27 nm was studied on silica surface with low to high surface coverage of NRs. The study was carried out to investigate both the dependence of the SERS intensity on the number of NRs and the NRs spacing on the silica surface. SERS of adsorbed molecules such as 2-aminothiophenol (2-ATP) and the capping molecules (hexadecyltrimethylammonium bromide) was studied on these surfaces using a near-IR laser excitation source (1064 nm). To produce silica surfaces covered with NRs, two approaches were used. In the first approach, monodispersed NRs gradually deposited from solution to silica surface and their number was increased by increasing the deposition time. In the second one, the NRs were first aggregated in solution and then deposited on the surface. Although using the first approach it was possible to prepare surfaces with high NR surface coverage, SERS intensity was found to be stronger for adsorbed molecules on surfaces covered with aggregated NRs. The observed increase in the SERS intensity in the case of aggregation was attributed to the enhancement of the electric field between the particles in the aggregates. It is shown that aggregated NRs in comparison with aggregated nanospheres (NSs) have stronger SERS enhancement under similar experimental conditions. In this comparison, some of the enhanced vibrational bands of 2-ATP on aggregated NRs are weakly enhanced or absent on aggregated NSs. Monitoring the SERS intensity of adsorbed 2-ATP versus its exposure time to the aggregated NRs shows that the SERS intensity of the adsorbed molecules reaches saturation, whereas the peak intensities of the capping molecules remain unchanged. The intensity saturation was discussed in terms of factors such as the saturation of the SERS active sites for 2-ATP on the gold surface and the partial damping of the plasmon band due to the stronger interaction of the adsorbate molecules with the metal surface.

### Introduction

It is known that the optical excitation of the surface plasmon band in an ensemble of individual colloidal metal nanoparticles can result in a significant increase in the average electromagnetic field intensities at the surface of the particles.<sup>1</sup> This enhancement, however, decreases as the excitation wavelength is shifted away from the surface plasmon absorption band.<sup>2</sup> In the case of ensembles of particles in aggregated form, where the plasmon modes can interact,<sup>3</sup> it is predicted that the excitation energy is not distributed uniformly over the particles but is localized in "hot spots", often much smaller than the excitation wavelength.<sup>4</sup> In surface-enhanced Raman scattering of molecules adsorbed on these surfaces, extraordinary enhanced Raman signals were observed in single molecule experiments and were attributed to the adsorption of the molecules at the hot spots located on the clusters of particles.<sup>5</sup>

In surface-enhanced Raman scattering (SERS) studies of bulk colloidal metal particles, Creighton et al.<sup>6</sup> originally exploited the effect of aggregation on the SERS activity of spherical silver particles. For the aggregated silver sol, the Raman excitation profile turned out to be coincident with the collective plasmon band in the red region of the spectrum. This supported the presence of the electromagnetic effect in the observed SERS

activity. In fact, all of the pronounced SERS activities in spherical particles under excitation wavelengths far from their normal surface plasmon band are attributed to the effect of the presence of the collective surface plasmon resonance<sup>7</sup> in aggregated particles.

Because of the anisotropy in their dimensions, gold NRs possess two types of surface plasmon bands, which are due to the coherent motion of the conduction band electrons along the short and long axis of the particle. The aspect ratio of the NR can be changed so as to change the wavelength of the surface plasmon band maximum from the visible to the near-IR region of the spectrum. In an earlier study of SERS activity of gold NRs<sup>8</sup> with a longitudinal plasmon band maximum at 700 nm and NSs with a plasmon band maximum at 520 nm under near-IR excitation wavelength of 1064 nm, it was shown that only NRs have very strong SERS activity. The reasons for this distinct behavior in NRs were the partial excitation of the longitudinal surface plasmon band and the contribution of the chemical effect due to the stronger binding of the adsorbate to the {110} facets of the NRs.

The SERS intensity depends on the concentration of adsorbed individual NRs to the silica surface and to the number of closely touched NRs, which possess possible SERS active sites at their junctions. In this study, the attempt has been to investigate the strength of the SERS intensity of the adsorbates due to the aforementioned factors. Therefore, the SERS intensity of the adsorbed molecules on NRs was monitored as the number of NRs on the silica surface was increased and compared with that

<sup>†</sup> Part of the special issue "George S. Hammond & Michael Kasha Festschrift".

\* To whom correspondence should be addressed. Phone: 404-894-0292. Fax: 404-894-0294. E-mail: mostafa.el-sayed@chemistry.gatech.edu.

of the molecules on the aggregated NRs. This comparison was carried out at a constant concentration of the adsorbate. Two strategies were followed to produce surfaces with high concentration of gold NRs. In the first, NRs were deposited from the solution to the silica surface in the absence of aggregation. The NR deposition time was increased to increase the number of NRs on the silica surface. In the second strategy, freshly aggregated NRs in solution were deposited on the silica surface. For aggregated NRs on the silica surface, the change in the SERS intensity versus the surface coverage of the adsorbate was studied. The SERS activity on aggregated NRs was also compared with the well-known SERS activity of aggregated nanospheres.

## Experimental

**Preparation of Gold NRs and NSs.** Surfactant-capped NRs with a plasmon band at 720 nm were prepared using a modified version<sup>9</sup> of the seed/growth method.<sup>10</sup> The cationic surfactant used was hexadecyltrimethylammonium bromide (CTAB). Based on TEM analysis, the average length and width of NRs were 27 and 10 nm, respectively. Citrate-capped gold NSs with a diameter of 12 nm were synthesized according to the method developed by Sutherland.<sup>11</sup>

**Preparation of Silica-NR Substrate.** The silica films with dimensions of 6 by 7 mm and a thickness of 100 micron were kept in 1 mL of a NR solution (7 nM) for 30, 60, 120, 240, and 360 s and afterward dipped into deionized water to wash out the loose NRs and surfactants.

**Preparation of the Silica-Aggregated NR Substrate.** For preparing aggregated NRs on a silica film, three drops of absolute ethanol were added to 1 mL of 7 nM NR solution (which also causes dilution of the NR solution to about 5 nM). The alcohol decreases the solubility of the particles and causes aggregation.<sup>12</sup> The color of the solution changed in seconds, and the aggregation process completed in less than 4 min. While aggregation was in progress, four silica films were consecutively inserted into the solution for 1 min. The slides were air-dried and were later exposed to 2-ATP solution.

**Preparation of the Silica-Aggregated NS Substrate.** An aggregated NS solution was prepared by adding a few drops of absolute ethanol to 1 mL of a 15 nM freshly prepared citrate-capped NS solution.<sup>13</sup> No further activation by adding anions such as chloride<sup>14,15</sup> was carried out. The effect of the halide ions in SERS activity will be addressed in the discussion section. Aggregated NSs were deposited on a silica film, by submerging a silica film into the solution of aggregated NSs for 2 min. The NS adsorption to silica is not efficient because of the charge similarity of the negatively charged NSs and the silica film. Therefore, drops of the aggregated NSs solution were deposited on the film, and the SERS signal was monitored after each addition. Addition of aggregated NSs was continued until the highest SERS signal was obtained. For all of the samples (in dried form), the visible reflection spectra was collected before and after film submersion into 0.2 mL of 0.005 M 2-aminothiophenol (2-ATP) in ethanol. After each immersion step in 2-ATP solution, the sample was left to dry to avoid the presence of alcohol peaks in the SERS spectrum. In the absence of aggregation, the number of deposited gold NRs on the silica film was calculated as described previously.<sup>8</sup>

**Instrumentation.** SERS spectra were collected using a FT-Raman spectrometer (Magna-IR accessory attached to a Nicolet 860 FTIR) in a 180° reflective configuration using a 1064 nm Nd:YAG laser source. In all the performed experiments, the laser power was 0.96 W. The NR-silica substrates were

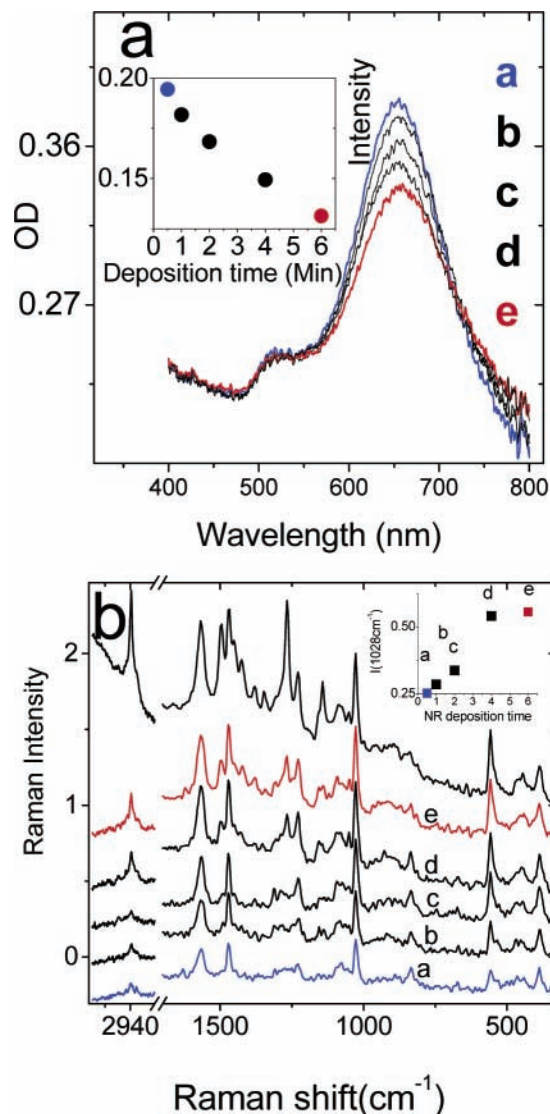


**Figure 1.** (a) From top to bottom: Visible reflection spectra of 5 NR-silica films after submerging in a 7 nM NR solution for 0.5, 1, 2, 4, and 6 min. The inset shows the decrease in the plasmon maximum intensity by increasing the deposition time. (b) From bottom to top: the first five SERS spectra belong to slides a, b, c, d, and e, respectively, which are exposed to 2-ATP for 20 min. The top spectrum belongs to the aggregated NRs.

positioned perpendicular with respect to the excitation source. The spectral resolution in Raman experiments was  $8 \text{ cm}^{-1}$ . For samples supported on silica film, visible reflection spectra of the dried films were collected using integrating sphere assembly of the Shimadzu spectrometer model UV-3101PC.

## Results

Upon introducing silica film to a gold NR solution, the NR adsorption to the silica surface starts. In the first approach, the NR concentration on the silica surface was added by increasing the film submersion time in the NR solution, which resulted in higher NR surface density and thus NRs with closer spacing. Figure 1a shows the visible reflection spectra of the prepared silica-NR films after insertion into a 7 nM NR solution for 0.5, 1, 2, 4, and 6 min, which are labeled as a, b, c, d, and e, respectively. The plasmon maximum of the dried films blueshifts about 70 nm relative to that of the NRs in solution or on wet films. The inset of Figure 1a shows that by increasing the deposition time the intensity of the plasmon band decreases,

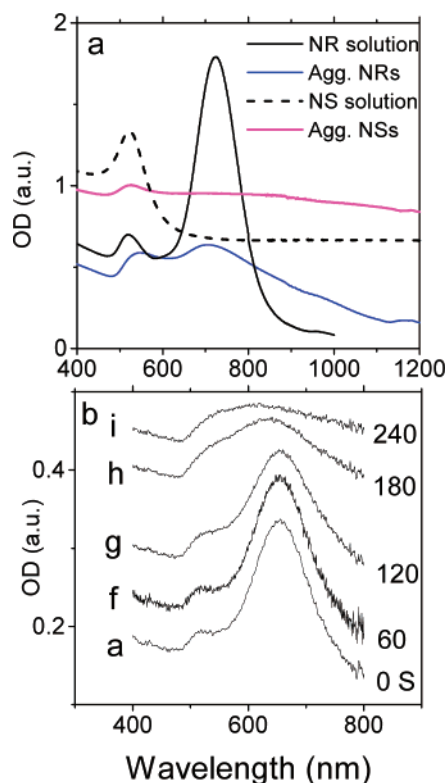


**Figure 2.** (a) Visible spectra of NR and NS solutions before and after inducing aggregation by alcohol. The drop of the dipolar plasmon band and rise of the collective plasmon modes over aggregate for both NRs and NSs can be seen in the lower energy. (b) Visible reflection spectra of NR-silica films at different stages of aggregation. Each film was submerged in solution for 1 min.

whereas it is expected to increase. In addition, the full width at half-maximum of the sample with the shortest deposition time (curve a) seems to be less than that of the sample with the longest submersion time (curve e). The decrease in the intensity of the longitudinal plasmon band (normal dipolar modes) is most likely due to the stronger interaction of the NRs on silica as they get closer to each other. The closeness of NRs is affected by the electrostatic repulsion between NRs due to their positively charged surface.

2-Aminothiophenol was attached to the gold surface by submerging the films in 200  $\mu\text{L}$  of 0.005 M 2-ATP ethanolic solution for more than 2 h. The SERS spectra of the films were collected at definite time intervals until the change in the peak intensity reached a steady state. Figure 1b shows the SERS spectra of the adsorbed 2-ATP molecules on the above films after 20 min immersion in the 2-ATP solution. The inset shows the peak intensity of the  $\delta(\text{C-H})$  vibration ( $1027\text{ cm}^{-1}$ ), which increases from films a to e.

In the second approach, aggregation was induced in a NR solution by addition of absolute ethanol, which resulted in a change of color of the solution in few seconds. Figure 2a shows the visible reflection spectra of NRs before and after adding ethanol (black and blue solid lines, respectively). The small and large clusters of NRs, which are made of in-touch NRs, were then deposited on the silica films. The visible spectra of these films in dried form are shown in Figure 2b, which also shows the progress of aggregation. The two distinct plasmon bands of the NRs merge to one very broad band upon aggregation. The color of the aggregated solution remains faint blue for about 1 h and the solution becomes colorless upon precipitation of the aggregated particles. In Figure 1b, curve i shows the SERS spectrum of the adsorbed 2-ATP molecules on the aggregated

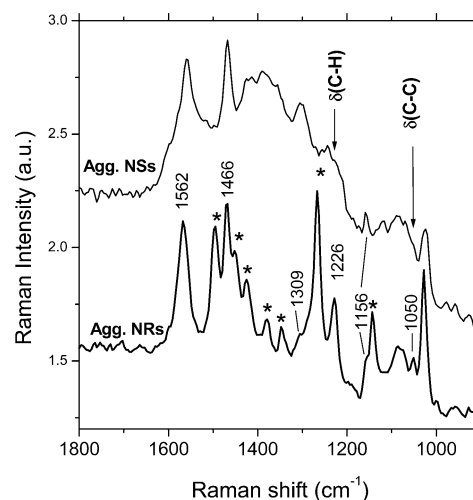


**Figure 3.** Comparison of the SERS activity of NRs and NSs deposited on silica. In NRs, the enhanced peaks are due to the capping material (labeled with stars) and adsorbed 2-ATP. For NRs and NSs, the submersion times in 2-ATP solution were 20 and 120 min. The assigned peaks belong to SERS of 2-ATP, which are only present in the aggregated NRs. In both cases, alcohol was used for inducing aggregation. The baselines have been shifted for clarity.

sample (visible spectrum is shown in Figure 2b, curve i). It can be seen that this film produces the highest intensity relative to other films.

The SERS intensities of 2-ATP adsorbed on the aggregated NRs and NSs were compared with each other. Two substrates were prepared by submerging silica films into aggregated solutions of NRs and NSs for 2 min. In deposition of individual NRs and NSs on silica, visible spectra of the prepared films indicated that, within 2 min of deposition time, the concentration of the adsorbed NRs to the silica is larger than that of NSs. This is due to the higher affinity of NRs to the silica surface, because of the positively surface charges of NRs. Furthermore, the rates of aggregation of NRs and NSs are expected to be different. Therefore, it is difficult to quantify the concentrations of the aggregated NRs and NSs on the silica. Consequently, their SERS comparison would be accompanied by a considerable amount of error. Because of the less efficient deposition of NSs to silica surface upon submersion, more NSs were deposited on the silica film by constant addition of freshly aggregated NSs to the silica surface until the SERS intensity reached its maximum value. The SERS spectrum shown in Figure 3 (top curve) belongs to 2-ATP molecules adsorbed on an aggregated NS film with the above description.

The 2-ATP adsorption rate to the gold surface in NRs and NSs could be different because of their different crystal structure. Gold NRs, in addition to the  $\{111\}$  and  $\{100\}$  facets, have a  $\{110\}$  facet, which has a higher surface energy.<sup>16</sup> This facet is absent in gold NSs. The results show that molecules bind more strongly to this facet relative to the other two facets.<sup>17</sup> Because the rate of 2-ATP adsorption is not known for these two particles and because of the weaker Raman peaks in the case of aggregated NSs, the film with the aggregated NSs was kept in the 0.005 M 2-ATP solution for a longer time (2 h). At a longer time, the concentration of the adsorbed molecules to the gold surface reaches its equilibrium value, although this could still be less than that for the NRs. In Figure 3, the enhanced peaks of adsorbed 2-ATP on NSs are obtained under the condition mentioned above and are compared to those on the aggregated NRs submerged in a 0.005 M 2-ATP for 20 min. Based on Figure 3 and the results above, it seems that NRs have stronger SERS activity relative to NSs.

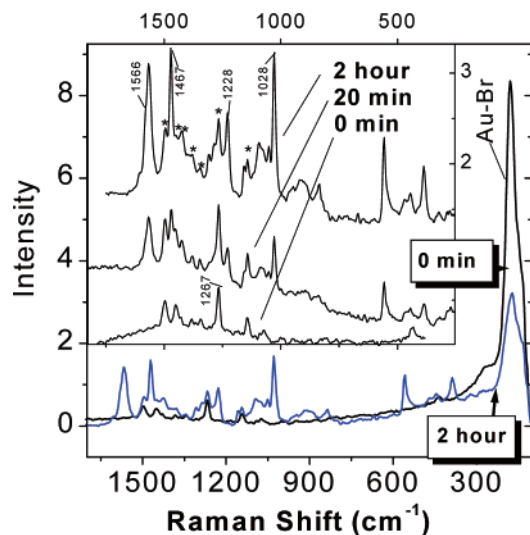


**Figure 4.** SERS of the capping molecules (CTAB) on aggregated gold NRs (before exposure to 2-ATP) (black curve). The blue curve is the same substrate after 2 h exposure to a solution of 0.005 M 2-ATP, rise of new peaks and fall of Au-Br vibration can be seen. Inset: SERS on aggregated NRs. The bottom, middle, and top curves are the same slide after 0, 20, and 120 min exposure to 2-ATP.

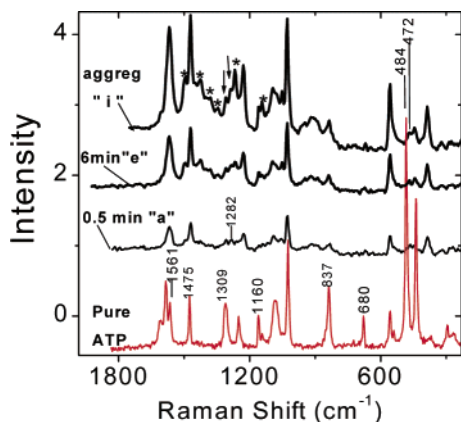


**Figure 5.** SERS of 2-ATP on different NR slides. From top to bottom: Film i (aggregated NRs), film e (6-min NR deposition), film a (0.5 min NR deposition time), the Raman spectrum of pure 2-ATP in the liquid phase. The bottom two spectra were used in calculating the enhancement factor in the absence of aggregation. Peaks labeled with stars belong to the capping molecules.

In both samples, peaks at 1466 and 1560  $\text{cm}^{-1}$  (which belong to C-C stretching modes) have comparable intensities. The peak at 1560  $\text{cm}^{-1}$  shows a redshift relative to the same vibration in NRs. In Figure 3, the 2-ATP peaks at 1226 and 1050  $\text{cm}^{-1}$  in the aggregated NRs have much lower intensities relative to those in the aggregated NSs. In the aggregated NRs, the  $\nu(\text{C}-\text{N})$  stretching mode at 1309  $\text{cm}^{-1}$  is not well resolved relative to the same peak in NSs. This is due to the overlap of this peak with the shifted  $\nu(\text{C}-\text{N})$  mode at 1280  $\text{cm}^{-1}$ . The peak at 1280  $\text{cm}^{-1}$  results from the binding of some of the nitrogen atoms of 2-ATP molecules to the gold surface. These two peaks can be seen clearly (two arrows in Figure 5) at higher 2-ATP surface coverage. Overall, most of the 2-ATP peaks can be seen in both cases although the intensities are different.

The continuum background seen in the spectrum of NSs looks similar to what has been reported by Brus' group,<sup>18</sup> although in their report the excitation wavelength was close to the dye absorption band and the normal plasmon band of NSs. The continuum has been attributed to the emission of a plasmon quantum with lower energies relative to the plasmon band

energy. These pairs are excited by the lower energy electrons, which have tunneled back from the LUMO of the adsorbed molecules to the metal particle. We observe strong SERS on NRs, whereas the continuum is weaker. In NSs, we do not observe strong SERS but the continuum is stronger. This might be a difference in exciting the continuum in the two systems.

## Discussion

On the substrate, the increase in the SERS intensity depends on three factors, i.e., the NR concentration, the number of clusters of aggregated NRs, and the concentration of the adsorbed 2-ATP molecules on active sites. The inset of Figure 1a shows that by increasing the NR deposition time, the plasmon intensity decreases while the SERS intensity of the corresponding substrate increases (inset of Figure 1b). A closer look at curve e in Figure 1a shows a slight rise of the red shoulder of the plasmon band (6 min deposition), which implies increase in the interaction between NRs.

Figure 2a shows that by increasing the extent of aggregation the extinction due to the dipolar modes (at 720 nm) decreases, whereas the extinction in the red region of the spectrum increases. The new adsorption in the red region results from the interaction of NRs in the aggregates. This means that NRs remain polarizable as the thin organic shell around particles prevents electrical contact between them.<sup>19</sup> In Figure 1b, comparison of the SERS spectra of the substrates a, b, c, d, and e with that of substrate i, shows that only in the latter case, the extent of aggregation is significant. This is consistent with its visible spectrum (Figure 2b, curve i). Spectrum i in Figure 1b suggests that, in the case of aggregation, the adsorbed molecules experience a much stronger field.

In spherical metal nanoparticles, it is known that the average electromagnetic field intensities at the surface of individual particles at the plasmon resonance become significant.<sup>1</sup> In the aggregated form, when particles are in close interaction, these fields can be enhanced further and localized in small regions (hot zones) of the fractal structure of the aggregate.<sup>20,21</sup> In NRs, theory predicts stronger field enhancement on the individual NRs.<sup>22</sup> In aggregated form, this enhancement is further increased when rods are in touch,<sup>23</sup> which is consistent with the above results.

### Effect of 2-Aminthiophenol Surface Coverage on SERS.

In Figure 4, the black spectrum belongs to the film i, which is coated with aggregated NRs capped with CTAB. The strong peaks related to the C-C stretching and bending modes of the CTAB methylene chains are seen in the 1000–1500  $\text{cm}^{-1}$  region of this spectrum. After 20 min exposure of this film to 0.005 M 2-ATP solution, spectrum changes to the blue curve shown in Figure 4. The intensity of the Au-Br vibration (174  $\text{cm}^{-1}$ ) decreases to less than half of its initial value and new peaks due to 2-ATP vibrations appear which are listed in Table 1.

By increasing the exposure time, the 2-ATP peak intensities such as 1566, 1467, 1228, and 1028  $\text{cm}^{-1}$  increase, whereas those of the capping molecules (for instance at 1267  $\text{cm}^{-1}$ ) remain almost constant (Figure 4, inset).

CTAB (capping material) binds to the gold surface via a Br<sup>-</sup> ion as a bridge (between the quaternary nitrogen and the gold surface),<sup>24</sup> whereas the majority of the 2-ATP molecules are adsorbed via their nitrogen and sulfur atoms. This conclusion is based on the facts that the in-plane vibrations  $\nu(\text{C}-\text{N})$  at 1309  $\text{cm}^{-1}$  and  $\nu(\text{C}-\text{S})$  at 484  $\text{cm}^{-1}$  have been shifted to 1282 and 472  $\text{cm}^{-1}$ , respectively, and weakly enhanced after 2-ATP adsorption to the gold surface (Figure 5).

**TABLE 1: SERS/Raman Peak Assignments of 2-Aminothiophenol Adsorbed on Gold NRs at 1064 nm Excitation Wavelength<sup>14a</sup>**

vibration	Raman pure 2-ATP $\pm 4 \text{ cm}^{-1}$	SERS $\pm 4 \text{ cm}^{-1}$	$E_{0.5\text{min}}$ $\pm 0.02$ (symmetry)	$EF_{0.5\text{min}}$ $\pm 0.6$	$E_{\text{agg}}$	$R_{\text{agg}}=$ $E_{\text{agg}}/E_{0.5\text{min}}$	$R_2=$ $E_{2\text{min}}/E_{0.5\text{min}}$	$R_6=$ $E_{6\text{min}}/E_{0.5\text{min}}$	$R_{\text{agg}}/R_2$	$R_{\text{agg}}/R_6$
$\gamma(\text{C-N})$	262	not found	— (A'')							
$\delta(\text{C-S})$	370	386	1.6 (A')	$6 \times 10^5$	4.3	$2.5 \pm 0.01$	$1.1 \pm 0.2$	$1.8 \pm 0.3$	$2.2 \pm 0.3$	$1.4 \pm 0.2$
$\gamma(\text{C-C})$	439	444	0.05(A'')		0.14	$2.3 \pm 0.4$	$1.0 \pm 0.1$	$1.6 \pm 0.2$	$2.2 \pm 0.3$	$1.5 \pm 0.4$
$\nu(\text{C-S})$	484	472	0.03 (A')		0.07	$1.3 \pm 0.5$	$1.0 \pm 0.1$	$1.1 \pm 0.3$	$1.4 \pm 0.5$	$1.4 \pm 0.4$
$\delta(\text{C-C})$	558	556	0.5(A')	$2 \times 10^5$	1.7	$3.4 \pm 0.05$	$1.2 \pm 0.2$	$2.4 \pm 0.2$	$2.6 \pm 0.3$	$1.4 \pm 0.2$
$\delta(\text{C-C})$	680	672	0.08 (A')		0.2	$2.3 \pm 0.1$	$0.9 \pm 0.2$	$0.6 \pm 0.05$	$2.4 \pm 0.4$	$1.4 \pm 0.2$
ring breathing	837	834	0.15 (A')	$6 \times 10^4$	0.43	$1.6 \pm 0.7$	$1.1 \pm 0.02$	$1.6 \pm 0.3$	$1.3 \pm 0.5$	$1.3 \pm 0.3$
$\delta(\text{C-H})$	1023	1027	0.3 (A')	$1 \times 10^5$	1	$2.6 \pm 0.7$	$1.0 \pm 0.02$	$2.0 \pm 0.1$	$2.4 \pm 0.4$	$1.5 \pm 0.1$
$\delta(\text{C-C})$	1050	1050	0.9(A')	$4 \times 10^5$	3	$3.3 \pm 0.8$	$1.3 \pm 0.07$	$2.4 \pm 0.2$	$2.5 \pm 0.4$	$1.6 \pm 0.2$
$\delta_{\text{as}}(\text{NH}_2)$	1073	1078	0.15 (A')	$6 \times 10^4$	0.8					
$\delta(\text{C-H})$	1160	1160	0.15 (A')	$6 \times 10^4$	0.8	$4.0 \pm 1$	$1.3 \pm 0.1$	$2.9 \pm 0.5$	$3.1 \pm 0.6$	$1.6 \pm 0.6$
$\delta(\text{C-H})$	1250	1226	0.6 (A')	$2 \times 10^5$	2.6	$3.8 \pm 0.4$	$1.2 \pm 0.1$	$2.5 \pm 0.2$	$3.2 \pm 0.2$	$1.6 \pm 0.1$
$\nu(\text{C-N})$	1309	1282	0.2 (A')	$8 \times 10^4$	0.8	$3.4 \pm 0.3$	$1.2 \pm 0.2$	$2.0 \pm 0.2$	$2.7 \pm 0.3$	$1.7 \pm 0.2$
$\nu(\text{C-N})$	1309	1309	0.2 (A')	$8 \times 10^4$	1	$3.6 \pm 0.1$	$1.3 \pm 0.2$	$2.4 \pm 0.3$	$2.7 \pm 0.2$	$1.7 \pm 0.6$
$\nu(\text{C-C})$	1475	1471	0.5 (A')	$2 \times 10^5$	2.3	$3.9 \pm 0.4$	$1.2 \pm 0.02$	$2.6 \pm 0.4$	$3.1 \pm 0.2$	$1.6 \pm 0.1$
$\nu(\text{C-C})$	1581, 1561	1562	— (A')							
$\delta_{\text{s}}(\text{NH}_2)$	1607	not found								

<sup>a</sup> EF, enhancement factor;  $E$ , ratio of  $I_{\text{SERS}}/I_{\text{Raman}}$ . For instance,  $E_{0.5\text{min}}$  is the enhancement factor for NR-silica sample with 30 s submersion time in NR solution.  $E_{\text{agg}}$ ,  $I_{\text{SERS}}/I_{\text{Raman}}$  of the aggregated NRs. The immersion time of the NR-silica substrate in the 2-ATP solution was the same for all the samples above and equal to 120 min.

The unshifted  $\nu(\text{C-N})$  mode at  $1309 \text{ cm}^{-1}$ , for adsorbed 2-ATP, also indicates that some of the nitrogen atoms are not bound to the gold surface. The lower degree of enhancement is also observed for in-plane vibrations such as  $\nu(\text{C-C})$  at  $1581$  and  $1561 \text{ cm}^{-1}$ , and  $\gamma(\text{C-C})$  and  $\gamma(\text{C-H})$  bending modes at  $680$  and  $1160 \text{ cm}^{-1}$ , respectively (Table 1). Among the out-of-plane vibrations,  $\gamma(\text{C-C})$  is observed at  $444 \text{ cm}^{-1}$ ; however,  $\gamma(\text{C-S})$  at  $170 \text{ cm}^{-1}$  overlaps with Au-Br vibration, which makes the assignment difficult. The weaker enhancement for the in-plane modes and the stronger enhancement for out-of-plane modes are signs of orientation of the plane of the molecule parallel to the particle surface. However, the presence of the ring-breathing mode at  $837 \text{ cm}^{-1}$  suggests a slight off parallel orientation. There are also some in plane bending modes such as  $\delta(\text{C-S})$ ,  $\delta(\text{C-C})$ , and  $\delta(\text{C-H})$  at  $370$ ,  $558$ , and  $1023$ , respectively, which have been strongly enhanced (Table 1) and are against a flat-on position. Overall, it seems the enhanced peaks above are more consistent with a molecular orientation between the two limits of the edge-on and the flat-on positions.

Based on the argument above as well as the decrease in the Au-Br peak intensity at  $174 \text{ cm}^{-1}$  (Figure 4, curves at 0 and 2 h), the Br ion cannot be between the adsorbed molecule and the gold surface, though the peak intensities of 2-ATP are much stronger relative to those of CTAB. This suggests that the active sites on the gold surface are not limited to the sites adjacent to the bromide ions. Previously, in the study of R6G on silver sol, Hildebrandt et al.<sup>14</sup> made a different conclusion. They suggested two types of adsorbing sites, specific and nonspecific on silver surface. In the site-specific case, the anion (halide ions) and the molecule form a complex with silver adatoms. They concluded that this type of site shows 100 times stronger enhancement.

Upon increasing the surface coverage, the peak intensities become independent of exposure time to 2-ATP molecules. Figure 6a shows the change in the peak intensity of the  $1027 \text{ cm}^{-1}$  vibration ( $\delta(\text{C-H})$ ) versus the exposure time of all of the NR-silica films to 2-ATP solution. These samples are different in their gold NR concentration, though the saturation time for all the samples is similar. Comparison of the visible reflection spectra of the samples before and after the adsorption of the 2-ATP molecules show decrease in the plasmon intensity and a slight red shift of the plasmon band (probably due to the partial

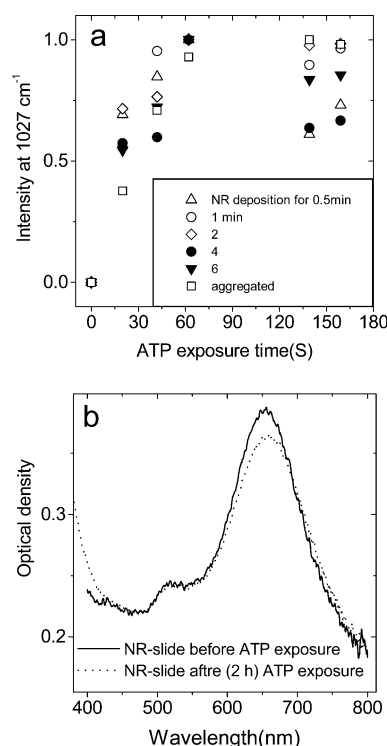


**Figure 6.** (a) Change in the peak intensity of  $1027 \text{ cm}^{-1}$  vibration upon increasing the exposure time to the 2-ATP 0.005 M solution. After about 1 h, the change in intensity slows down, which shows the saturation point. However, after 2 h, the peaks due to the capping material are still present in the SERS spectrum (see Figure 4). (b) The change in the visible reflection spectra after 2 h exposure to 2-ATP molecules. The damping in the plasmon is attributed to the adsorption of the cyclic thiol (see text).

change in the capping material). This behavior is shown in Figure 6b. One possible explanation for the decrease in the absorption band could be the deterioration of the NRs in the presence of the 2-ATP molecules. This could result in SERS signal saturation or even its decrease.

Saturation and decrease in the SERS intensity has been reported previously. For instance, Murray et al.<sup>25</sup> in the study of the cyanide surface coverage and Pockrand et al.<sup>26</sup> in the study of the pyridine surface coverage on silver-island films

have observed SERS intensity saturation and red shift in the extinction spectrum of the substrate upon increasing the surface coverage of the adsorbed molecules. Murray et al. have related this behavior to the depolarization effect of the surrounding molecules of a given molecule. Otto et al.<sup>27</sup> have also tentatively attributed the SERS intensity saturation to the shift in the affinity levels (adsorbed states) of the molecules to higher energy because of their dependence on the surface coverage. Another possibility for the intensity saturation could be due to the limited number of available sites for 2-ATP molecules on gold surface. Although Au–S bond formation is energetically the most favorable bond formation, it could be difficult for the 2-ATP molecules to completely replace all of the capping material bound to the {110} facet. This argument is consistent with the presence of the SERS peaks of the capping material even after exposing the substrate to 2-ATP solution for 2 h.

In Figure 6b, the decrease in the plasmon band intensity by increasing the adsorption of 2-ATP molecules could also be due to the damping of the plasmon oscillation leading to the broadening of its band. The damping of the plasmon band by introducing thiol groups has been reported in the past.<sup>28</sup> Based on the Persson's model,<sup>29</sup> individual ballistic electrons or holes generated via excitation of the surface plasmon could couple to the chemisorbed molecule. Depending on the orbital energies of the molecules relative to the Fermi level of the metal, weak or strong coupling between the excited electron–hole pairs of metals and adsorbed molecules could take place. This results in inelastic scattering of the electrons to metal.<sup>21</sup> The stronger SERS of the adsorbed 2-ATP molecules relative to the capping material is a reliable evidence of stronger interaction of the 2-ATP molecules with gold NRs. This stronger interaction could also result in stronger plasmon damping by the 2-ATP molecules relative to the original capping molecules (CTAB). This interaction increases the chance of inelastic scattering of the electrons at the metal/ligand interface, which results in faster relaxation of the plasmon excitation and broadening of the plasmon absorption band.<sup>30</sup> The decrease in the intensity of the plasmon band could also explain the loss of the Raman intensity at higher surface coverage.

**Estimating the Enhancement Factor in the Absence of Aggregation.** The SERS spectrum of the film with a 0.5-min NR deposition (film a) was used in determining the enhancement factor. The number of adsorbed NRs on the film was estimated based on the extinction coefficient and the optical density of the NRs at their plasmon band maximum at 650 nm. The adsorbed 2-ATP concentration on the NRs with an aspect ratio of 2.7 was calculated to be  $5.06 \times 10^{-6}$  M, assuming a monolayer of the 2-ATP molecules with a surface area of 28 Å on the gold surface. Using the above data and the peak intensities at 1027  $\text{cm}^{-1}$  (Figure 5), the enhancement factor for NRs was found to be about  $10^5$ , which was similar to the previously reported value.<sup>8</sup> These values are shown for different peaks in Table 1.

Figure 5 shows that in the aggregated NRs (film i) the peak intensities are stronger relative to those of the 6-min NR deposition (film e); however, there are no signs of evolution of new peaks. The relative peak enhancement was examined as a function of the degree of aggregation. This ratio could indicate whether the adsorbed molecules on the aggregated NRs experience a different environment relative to those adsorbed on individual NRs. The  $I_{\text{SERS}}$  for substrates with 2-min NR deposition (film c) and aggregated NRs (film i) were each divided by that of the substrate with 0.5-min NR deposition (these ratios are called  $R_2$  and  $R_{\text{agg}}$ , respectively). The  $R_{\text{agg}}/R_2$

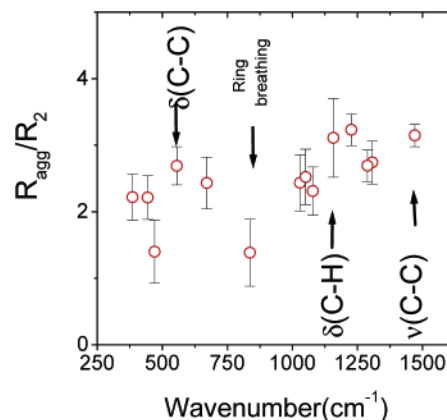


**Figure 7.** Relative peak enhancement in the aggregated sample  $R_{\text{agg}}/R_2$  for different vibrations of 2-ATP. The scattered points show that not all of the vibrations have been enhanced equally in the aggregated sample. This shows that some of the vibrations experience the field in a different way relative to the same vibration in the absence of aggregation.

and  $R_{\text{agg}}/R_6$  ratios (relative enhancement) are listed in Table 1. The  $R_{\text{agg}}/R_2$  values are also plotted versus the vibration energy in Figure 7. The obtained relative enhancement is 250% larger than that of the NR films prepared using the first approach (from monodispersed NRs). In the case of aggregation, the enhancement pattern of vibrations is different from that in the absence of aggregation. For all of the stretching modes, the relative enhancement is increased, whereas for some of the bending modes, this value is decreased. The change in the relative enhancement suggests that the field symmetry in the aggregate is different from that in the absence of aggregation and most of the SERS intensity in the aggregated sample originates from the molecules adsorbed on active spots in the aggregates and not on individual NRs.

Despite the  $R_{\text{agg}}/R_2$  ratio, the  $R_{\text{agg}}/R_6$  ratio is rather a constant number for all of the vibrations. This might mean that NRs in the substrate with a 6-min NR deposition has characteristics similar to the aggregated sample, but with fewer numbers of active sites (This is also suggested by the fact that the optical absorption spectrum of the 6-min NR deposition sample shows broadening, which is a sign of aggregation.). In the first approach, a larger number of NRs is required to produce SERS intensity comparable to the SERS of the aggregated sample. Longer NR deposition time does not greatly increase the SERS intensity; instead, it results in substrate instability (because of the melting of the NRs upon laser irradiation). It seems that the number of SERS active sites can be increased more efficiently by inducing aggregation. In the arguments above, it has been assumed that the adsorption rates of 2-ATP from solution to individual NRs or on aggregates of NRs are similar, as it might be diffusion controlled.

It would be difficult to estimate the absolute enhancement factor in aggregated NRs because the concentration of the adsorbed molecules is not known. It is not clear how many molecules are at junctions of particles and how many are adsorbed on the surface of individual particles. Samples i and a in Figure 5 are examples of aggregation and absence of aggregation, respectively, which were exposed to 2-ATP molecules under similar conditions. In sample a, we tried to increase the SERS intensity by adding more unaggregated NRs. Figure 5, shows the NR film after 6 min exposure to a NR solution (sample e). The peak intensities are larger than that of

the 1-min NR deposition time (sample a); however, the peak intensities never reach the level seen in the aggregated sample (sample i).

In comparing the two approaches, the strength of the second approach could be due to the smaller spacing between NRs. It could also be that the number of sites with close spacing (active) is larger in the second approach (aggregated NRs). A more quantitative enhancement factor requires near-field measurements and studies to find the contribution of the Raman scattering from these hot spots. However, no matter what type of configuration is considered for NRs in their aggregated form, e.g., side by side, end to end, or crossed, our results show stronger Raman enhancement in the case of aggregation. The adsorbed molecules in these junctions are most likely the origin of the observed increase in our SERS results. The above arguments and the  $10^5$ -enhancement factor in the absence of aggregation translate to a much stronger enhancement factor in the case of aggregated NRs, which introduces NRs as a new and strong rival for colloidal nanospheres in the SERS applications.

**Acknowledgment.** This study was funded by the material science division of the National Science Foundation Grant No. 0138391.

#### References and Notes

- (1) (a) Kerker, M.; Wang, D. S.; Chew, H. *Appl. Opt.* **1980**, *19*, 4159. (b) Flytzanis, C. *Prog. Opt.* **1992**, *29*, 2539.
- (2) Bright, R. M.; Musick, M. D.; Natan, M. J. *Langmuir* **1998**, *14*, 5695.
- (3) Fornasiero, D.; Grieser, F. *J. Chem. Phys.* **1987**, *87* (5), 3213.
- (4) Shalaev, V. M.; Botet, R.; Mercer, J.; Stechel E. B. *Phys. Rev. B* **1996**, *54* (11), 8235.
- (5) Kneipp, K.; Kneipp, H.; Kartha, V. B.; Manoharan, R.; Deinum, G.; Itzkan, I.; Dasari, R. R.; Feld, M. S. *Phys. Rev. E* **1998**, *57* (6), R6281.
- (6) Creighton, J. A.; Blatchford, C. G.; Albrecht, M. G. *J. Chem. Soc. Faraday Trans. 2* **1979**, *75*, 790.
- (7) Freeman, R. G.; Grabar, K. C.; Allison, K. J.; Bright, R. M.; Davis, J. A.; Guthrie, A. P.; Hommer, M. B.; Jackson, M. A.; Smith, P. C.; Walter, D. G.; Natan, M. J. *Science* **1995**, *267*, 1629.
- (8) Nikoobakht, B.; Wang, J.; El-Sayed, M. A. *Chem. Phys. Lett.* **2002**, *366*, 17.
- (9) Nikoobakht, B.; El-Sayed, M. A. *Chem. Mater.* In press.
- (10) Jana, N. R.; Gearheart, L.; Murphy, C. J. *J. Phys. Chem. B* **2001**, *105* (19), 4065.
- (11) Sutherland, W. S.; Winefordner, J. D. *J. Colloid. Interface Sci.* **1992**, *48*, 129.
- (12) Gold NSs were made by the method of Sutherland, W. S.; Winefordner, J. D. *J. Colloid. Interface Sci.* **1992**, *48*, 129.
- (13) Hildebrandt, P.; Stockburger, M. *J. Phys. Chem.* **1984**, *88*, 5935.
- (14) Griffith, W. P.; Koh, T. Y. *Spectrochim. Acta* **1995**, *51*, 253.
- (15) Liz-Marzan, L. M.; Giersig, M.; Mulvaney, P. *Langmuir* **1996**, *12*, 4329.
- (16) Wang, Z. L.; Mohamed, M. B.; Link, S.; El-Sayed, M. A. *Surf. Sci.* **1999**, *440*, L809.
- (17) Wang, Z. L.; Gao, R. P.; Nikoobakht, B.; El-Sayed, M. A. *J. Phys. Chem. B* **2000**, *104*, 5417.
- (18) Michael, A. M.; Nirmal, M.; Brus, L. E. *J. Am. Chem. Soc.* **1999**, *121*, 9932.
- (19) Kreibig, U.; Vollmer, M. *Optical Properties of Metal Clusters*; Springer: Berlin, 1995; pp 157.
- (20) Markel, V. A.; Shalaev, V. M.; Zhang, P.; Huynh, W.; Tay, L.; Haslett, T. L.; Moskovits, M. *Phys. Rev. B* **1999**, *59*, 10903.
- (21) Michaels, A. M.; Jiang, J.; Brus, L. *J. Phys. Chem. B* **2000**, *104*, 11965.
- (22) Wang, D. S.; Kerker, M. *Phys. Rev. B* **1981**, *24*, 1777.
- (23) Garcia, V. F. G.; Pendry, J. B. *Phys. Rev. Lett.* **1996**, *77*, 1163.
- (24) Koglin, E.; Tarazona, A.; Kreisig, S.; Schwuger, M. *J. Colloids Surf. A* **1997**, *123–124*, 523.
- (25) Murray, C. A.; Bodoff, S. *Phys. Rev. Lett.* **1984**, *52*, 2273.
- (26) Pockrand, I.; Atto, A. *Sol. State Commun.* **1980**, *35*, 861.
- (27) Otto, A.; Mrozek, I.; Grabhorn, H.; Akemann, W. *J. Phys. Condens. Matter* **1992**, *4*, 1143.
- (28) (a) Linnert, T.; Mulvaney, P.; Hengline, A. *J. Phys. Chem. B* **1993**, *97*, 679. (b) Hengline, A.; Meisel, D. *J. Phys. Chem. B* **1998**, *102*, 8364.
- (29) Persson, B. N. J. *Surf. Sci.* **1993**, *281*, 153.
- (30) Kreibig, U.; Vollmer, M. *Optical Properties of Metal Clusters*; Springer: Berlin, 1995; pp 300–301.